Malaysian Journal of Science **21A**: 83-86 (2002)

X-ray photoelectron spectroscopy for probing non-bridging oxygen in silver ion conductors and their relationship to ionic conductivity

E.B. Saniman[1], M.Z.A. Yahya[2] and A.K. Arof[3]

[1]*Material Science Program, Universiti Kebangsaan Malaysia, 43600 Bangi, Selangor. Malaysia.*
[2]*Physics Department, Faculty of Applied Science, MARA University of Technology, 40450 Shah Alam, Selangor, Malaysia.*
[3]*Physics Department, Faculty of Science, University of Malaya, 50603 Kuala Lumpur, Malaysia.*

ABSTRACT The materials studied in this work are $60AgI\text{-}20Ag_2O\text{-}20[0.1M_mO_n + 0.9M'_{m'}O_{n'}]$ of the boron oxide rich glass with M_mO_n as WO_3 and $M'_{m'}O_{n'}$ as B_2O_3 and the WO_3 rich glass with M_mO_n as B_2O_3 and $M'_{m'}O_{n'}$ as WO_3. XPS has shown that for glasses with the same amount of network modifiers glasses with a higher electrical conductivity have a larger number of (non-bridging oxygen) NBOs. This experiment helped in the deduction of the formation of tetrahedral oxyanions which when share corners with one another could result in the formation of larger channel-like pathways or "open structures" in the glasses through which more silver ions can flow through with ease.

(XPS, Silver glasses, Bridging oxygen, Non-bridging oxygen)

INTRODUCTION

While the structure and ion transport mechanism in crystalline materials are well understood, the structure-transport property relation in glasses is limited. This is mainly due to the disordered nature or the short range ordering of glasses, which prevents accessibility of detailed x-ray diffraction studies. The creation of structural disorder during fusion of the glasses on the other hand is considered to be responsible for the formation of high concentrations of defects, which lead to the greatly enhanced conductivities as compared to their crystalline counterparts. Hence there is a need to resort to other experimental techniques for obtaining defect and structural information, which cannot be avoided in order to establish structure-property relationships. Since x-ray photoelectron spectroscopy (XPS) is one of the important techniques that are widely used for studying surfaces of solid materials, we apply this apparently useful technique for studying the binding energy of non-bridging oxygens (NBOs) and bridging oxygens (BOs) [1] in silver ion conducting glasses such as $60AgI\text{-}20Ag_2O\text{-}20[0.9WO_3 + 0.1B_2O_3]$, the tungsten rich glass and $60AgI\text{-}20Ag_2O\text{-}20[0.1WO_3 + 0.9B_2O_3]$, the boron oxide rich glass.

EXPERIMENTAL

The materials were prepared by quenching the melt of the stoichiometrically weighed constituents at liquid nitrogen temperature. The XPS studies in this work were carried out using a Kratos HSI x-ray spectrometer with the Mg x-ray source (1253.6 eV), which is available at the Kratos Analytical (Manchester, United Kingdom). The spectrum was recorded at an operating current and voltage of 10 mA and 14 kV, respectively. The spectrometer was calibrated using a clean Ag plate and the Ag $3d_{5/2}$ line was set at 368.25 eV. The C 1s binding energy at 284.80 eV was used as a second reference. The solid polymer sample was mounted onto a standard stub holder using double-sided adhesive tape. The survey scan was recorded in the energy range between 10 eV to 1100 eV. The pass energy and step size energy was 160 eV and 1 eV $step^{-1}$ respectively. Sweep time was set at 300 seconds per sweep. For the narrow scan, smaller pass energy of 20 eV with lower step size, 0.1 eV $step^{-1}$ was utilized. The

sweep time was 59.898 seconds per sweep. Narrow scans were obtained for the C 1s, O 1s, N 1s, Zn 2p3/2, and Li 1s signals. The sample analysis chamber was kept at ≈ 5.0 x 10^{-9} torr or less during the scans. The vision software provided by Kratos deconvoluted all core-level spectra into gaussian component peaks. Charging effects were corrected for using the C 1s binding energy at 284.80 eV.

RESULTS AND DISCUSSION

In this investigation, we seek confirmation on the presence of boron oxyanions in the WO_3 rich glass i.e. $60AgI\text{-}20Ag_2O\text{-}20[0.9WO_3 + 0.1B_2O_3]$ and the presence of tungsten oxyanions in the boron oxide rich glass by looking at the B1s ($60AgI\text{-}20Ag_2O\text{-}20[0.9WO_3 + 0.1B_2O_3]$) and W4f photopeaks at the binding energy of approximately 190 eV and 35 eV respectively. Apart from that, bridging and non-bridging oxygens can also be differentiated and the quantity of these oxygens be estimated to explain the observation of higher ionic conductivity in the tungsten oxide rich glass. Figure 1 shows the survey spectrum (wide scan spectrum) for the tungsten oxide rich glass.

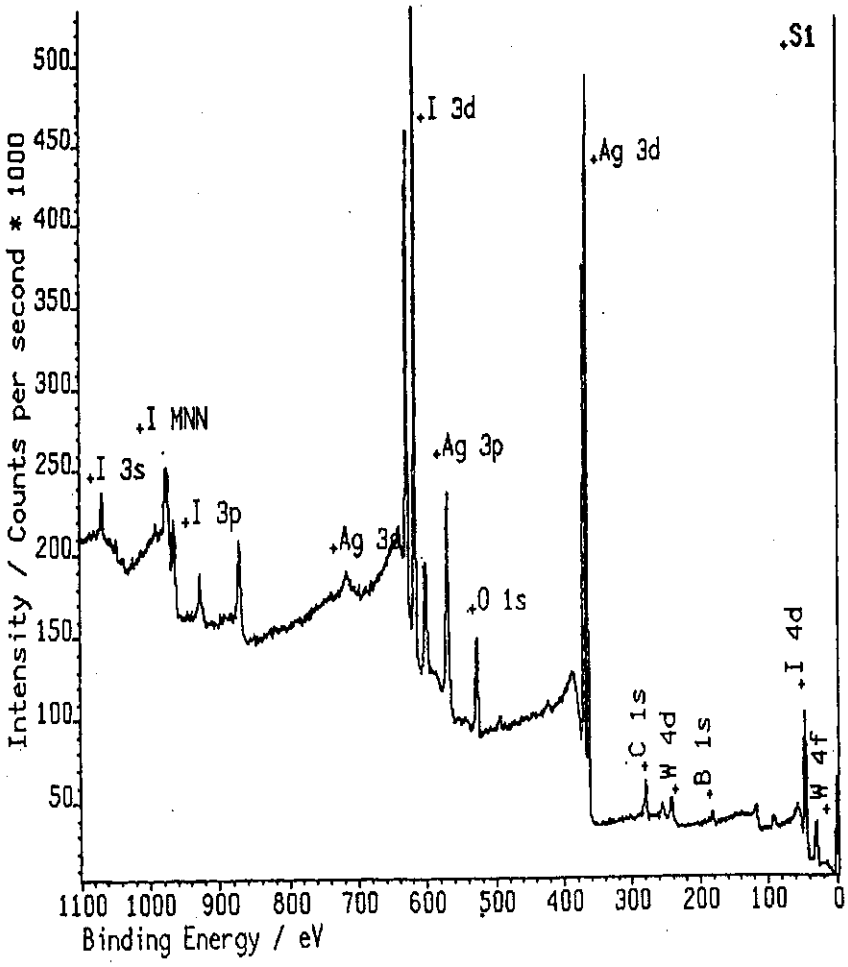

Figure 1. Wide scan spectrum for the silver borotungstate glass with the highest conductivity.

...urvey spectrum for the boron oxide rich ... also shows the photoelectron and Auger ... for the same elements. Table 1 lists some ...teristics of the peaks for the tungsten oxide ... glass and Table 2 lists some characteristics ... peaks for the boron oxide rich glass. The ...ic concentration of the elements was ...ulated by equation:

$$\text{atomic \% of element X} = \frac{(A_x / S_x)}{\sum_{i=1}^{n} (A_i / S_i)}$$

...llowing Chowdari [3], the O1s 1 peak is ...signed to non-bridging oxygen (NBOs). The O1s 2 peak is assigned to adventitious water and the O1s 3 peak is assigned to bridging-oxygen (BOs), Figure 2 (a) and (b). The ratio of BOs to NBOs is thus always lower than 1. Literature has shown [3] that the increase in NBOs lead to the increase in conductivity. The increase in NBOs is due to the network modifier rupturing the BO bonds between adjacent glass former tetrahedral and substituting them with NBOs. Hence the number of NBOs increases with modifier content. In this work, we have also shown that for a fixed modifier content, the material with the higher NBO to BO ratio still exhibits the higher conductivity.

...ble 1: XPS of $60AgI\text{-}20Ag_2O\text{-}2B_2O_3\text{-}18WO_3$. C1s binding energy = 284.80 eV [2].

Peak	Position BE/eV	FWHM/ eV	Raw Area	Sensitivity Factor	Atomic Concentration %
Ag3d	368.47	0.91	113730	2.160	34.27
...13d	619.87	1.03	95125	3.846	16.10
O1s 1	529.86	0.99	5085	0.287	11.53
O1s 2	531.16	1.44	3615	0.287	8.20
O1s 3	532.32	2.42	4010	0.287	9.09
...B1s	187.20	2.50	1635	0.056	19.00
...W4f	34.87	0.69	3398	1.219	1.81

Table 2: XPS of $60AgI\text{-}20Ag_2O\text{-}18B_2O_3\text{-}2WO_3$. C1s binding energy = 284.80 eV [2].

Peak	Position BE/eV	FWHM/ eV	Raw Area	Sensitivity Factor	Atomic Concentration %
Ag3d	368.69	0.85	113738	2.160	31.76
13d	619.99	1.00	104420	3.846	17.95
O1s 1	530.31	1.23	2338	0.287	5.39
O1s 2	531.36	1.46	4718	0.287	10.87
O1s 3	532.87	1.80	1850	0.287	4.26
B1s 1	187.33	2.81	2120	0.056	25.03
B1s 2	191.60	1.57	379	0.056	4.48
W4f	35.01	0.71	479	1.219	0.26

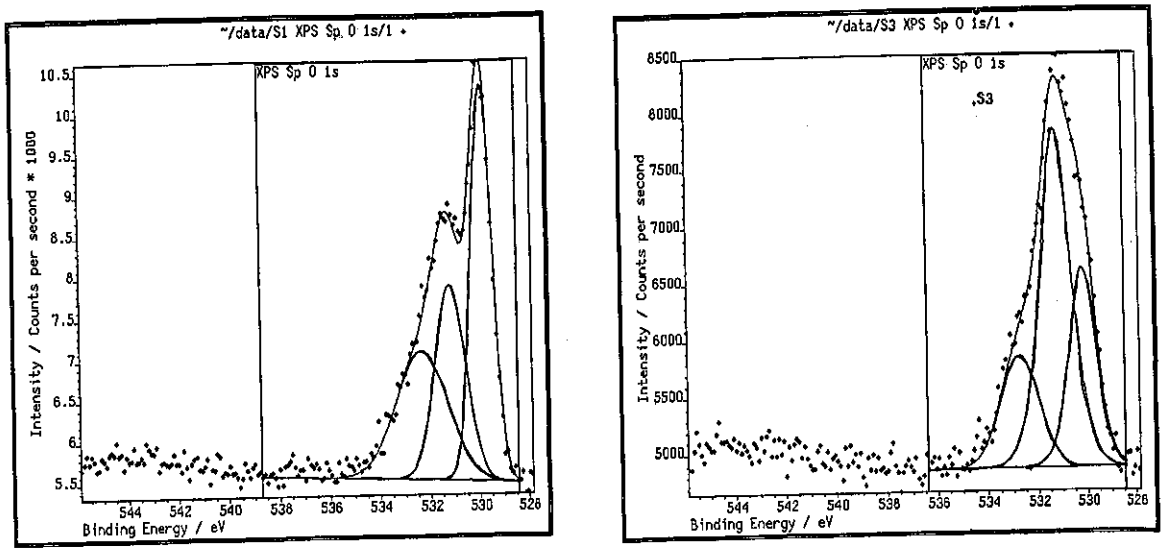

(a) (b)

Figure 2. O1s photopeak from XPS spectrum of (a) 60AgI-20Ag_2O-2B_2O_3-18WO_3 and (b) 60AgI-20Ag_2O-18B_2O_3-2WO_3

Following [3], the NBO:BO ratio for the tungsten oxide rich glass and for the boron oxide rich glass is 1.2681 and 1.2638 respectively. The room temperature electrical conductivity for the WO_3 rich glass is 3.8 x 10^{-2} S cm^{-1} and for the B_2O_3 rich glass is 1.9 x 10^{-2} S cm^{-1}. Within experiment error, even in the temperature range from 0 °C to 70 °C, the conductivity of the WO_3 rich glass is always about twice that of the B_2O_3 rich glass.

CONCLUSION

X-ray photoelectron spectroscopy (XPS) has confirmed the NBOs play a dominant role in the determination of the electrical conductivity of silver ion conducting glasses. Even for a small difference in NBO:BO ratio, the increase in conductivity is well manifested.

REFERENCES

1. Jen, J.S., Kalinowski, M.R. (1989). *J. Non-Cryst. Solids.* **38&39**: 21 - 26.
2. Chastin, J. (1992). *Handbook of X-ray Photoelectron Spectroscopy*, Perkin Elmer Corporation, USA.
3. Chowdari, B.V.R. (1990). *Recent Advances in Fast Ion Conducting Materials and Devices.* (eds) Chowdari, B.V.R., Liu, Q.G. and Chen, L.Q. World Scientific, Singapore: 55 – 62.

Malaysian Journal of Science **21A**: 87-95 (2002)

X-ray diffraction of residual stresses in boron nitride coated on steel substrate

E. Hamzah, R.D. Ramdan, V.C. Venkatesh and **N.H.B. Hamid**

Faculty of Mechanical Engineering, Universiti Teknologi Malaysia.

ABSTRACT Cubic boron nitride (cBN) is a promising coating material for cutting tools especially for applications that have contact with ferrous metals. This is because of its extreme hardness, chemical stability at high temperature and inertness with ferrous metals. However applications of cBN as coating material has not been used extensively due to the poor adhesion between cBN and its substrate. High stress level in the film is considered to be the main factor for the delamination of cBN films after deposition. Thus the present research concentrates on residual stress analysis of cBN films by X-ray diffraction method. Fourier transform infra-red (FTIR) spectroscopy analysis was also performed on the samples to study the structure of the deposited films. Based on the present experimental results and previous literature study, a new theoretical model for cBN film growth was proposed.

(Residual Stresses, Cubic Boron Nitride, X-Ray Diffraction)

INTRODUCTION

Research on boron nitride (BN) is a challenging field and has attracted a lot of attention. BN forms at least four distinct crystalline phases, namely cubic boron nitride, hexagonal boron nitride, wurtzite boron nitride and rhombohedral boron nitride[1]. Cubic boron nitride (cBN) and hexagonal boron nitride (hBN) are two forms of boron nitride, which had been extensively investigated with promising industrial applications. Cubic boron nitride has extreme properties, which make it to be an important material. This includes high hardness and thermal conductivity, wide band gap and ability to be doped both p-type and n-type [2]. In its equilibrium phase diagram, cBN forms under high pressures (> 10 GPa) at temperatures above 2000°C[2].

However applications of cBN as a coating material have not been extensively used due to its poor adhesion between cBN and the substrate. High stress level in the films is considered to be the main factor that caused the delamination of the cBN films after deposition. Thus study on the stress level of this films and its effect on cBN film adhesion is important. In addition, stress which is created in the films is also considered to be caused by cBN formation as reported by McKenzie *et. al* [3]. Similarly Windschman [4] also proposed that stress is caused by the volumetric distortion from the displaced atoms scales linearly with the energy, which is needed for transformation to cBN.

In this work, residual stress analysis in the films that have various forms of boron nitride structure including cubic form has been performed using X-ray diffraction method (XRD). There are two types of residual stresses, namely macroscopic residual stress, and microscopic residual stress. Macroscopic residual stress is responsible for the shift of the diffraction angle of diffraction lines while microscopic residual stress is based on the width or on the shape of the diffraction line. If x-ray residual stress analysis is mainly based on the angular shift of diffraction lines, the present work concentrates on the analysis of the macroscopic residual stress in the films.

MATERIALS AND METHODS

Boron nitride films were deposited on high speed steel (HSS) substrate using radio frequency (Rf) sputtering process with high purity (IC grade) boron nitride as the target material. Before the deposition process, steel substrates were ultrasonically cleaned in the acetone solution. Argon gas was used as the

working gas in the deposition chamber. The distance between substrate and target, substrate temperature (~ 25°C), Rf power, gas flow rate and pressure were fixed at 2.2 cm, room temperatures, 200 watts, 200 sccm and 0.04 mtorr respectively. In order to examine the film growth, deposition time was varied between 1 hour and 5 hours.

Residual stress analysis of the resulting films was calculated using computer software called DIFFRAC^{plus}. The angle 2θ value which was analyzed for stress measurement ranges from 130° to 140°.

For stress measurement, the ψ-tilting can be made in two ways. Firstly by the iso-inclination mode, which involves tilting within the area containing the primary and diffracted beams. Secondly is the side-inclination mode where inclination mode lies within an area perpendicular to the area containing the beam path. In the present work the iso-inclination mode was used to perform residual stress measurement. Figure 1 shows the orientation of strain components, $\varepsilon_{\varphi\psi}$, and stress components, σ_{φ}, with respect to the coordinate system, P_{11}, P_{22}, P_{33}, of the sample. Complete residual stress measurement parameters are given in the Table 1.

Fourier transform infra-red (FTIR) spectroscopy has been carried out for films structure analysis.

Table 1: Parameters for Stress Measurement by X-ray Method

Parameter	Value
Measurement Area (range of 2θ)	100-145°
Scan type	Inclination mode
2θ step	0.385
Azimuth phi settings	0,45,90°
Tilt psi settings	-45 up to 45 with 11° step size

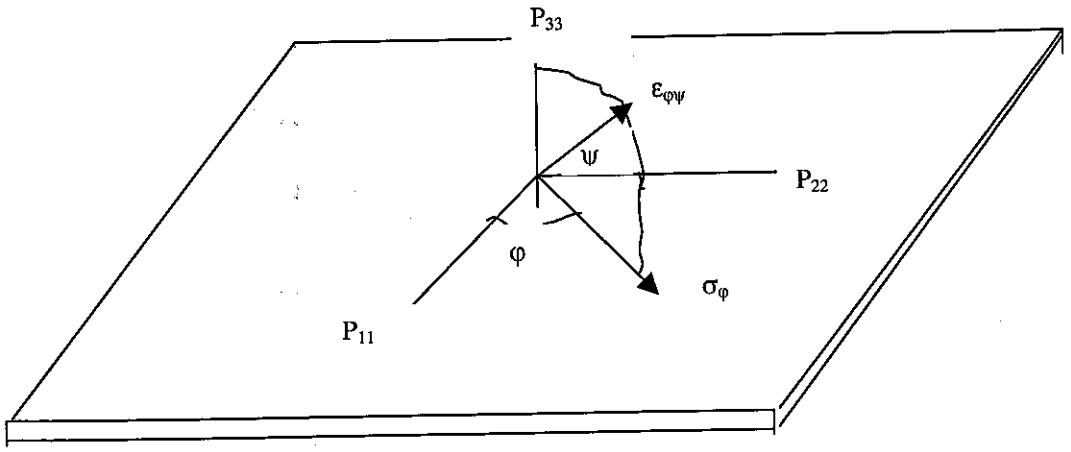

Figure 1. Orientation of $\varepsilon_{\varphi\psi}$ and σ_{φ} [5]

RESULTS AND DISCUSSION

Residual Stress Measurement

As mentioned earlier, there are two types of residual stresses that can exist namely microscopic and macroscopic residual stress, which may be present in the material. In this work, both analyses were performed.

In XRD the position of the diffraction angle is determined by lattice distance, d, and which correspond to 2θ (diffraction angle) value given by the Bragg law;

$$n\lambda = 2\, d \sin\theta \qquad \ldots\ldots\ldots\ldots\ldots(1)$$

where λ is the wavelength of the target source of XRD system, n is the number of internal spacing.

Figure 2 is a schematic diagram of interaction between X-ray and atoms in a crystal. If stress is present, lattice distance will be strained, thus d value will be changed and as a consequent the position of 2θ value (diffraction angle) will be shifted. In other words, the shift of the diffraction angle of the diffraction lines is an indication of stress in a material.

For homogeneous macroscopic stress state within an elastically isotropic volume, the relationship between the strain components, $\varepsilon_{\varphi\psi}$, measured via diffraction at angles φ, ψ and the stress component, σ_{ij} (which are in general related to the sample coordinate system, P_{ij}) is given by the theory of linear elasticity;

$$\varepsilon_{\varphi\psi} = \tfrac{1}{2} s_2 [\sigma_{11} \cos^2\varphi + \sigma_{12} \sin 2\varphi + \sigma_{22} \cos^2\varphi]\sin^2\psi + \tfrac{1}{2} s_2\, \sigma_{33} \cos^2\psi + s_1 [\sigma_{11} + \sigma_{22} + \sigma_{33}] + \tfrac{1}{2} s_2 [\sigma_{13} \cos\varphi + \sigma_{23} \sin\varphi] \sin 2\psi \qquad \ldots\ldots\ldots(2)$$

Based on Equation (2), residual stress in the boron nitride films was measured using DIFFRAC^{plus}.

Figure 3 is a typical graphical presentation of stress measurement of boron nitride films by XRD. Figure 3 correlates between $\varepsilon_{\varphi\psi}$ and $\sin^2\psi$ and which is based on Equation (2).

Stress tensor in MPa for samples with different deposition time is listed in Table 2 which summarizes the stress shown in Figure 4 and Figure 5.

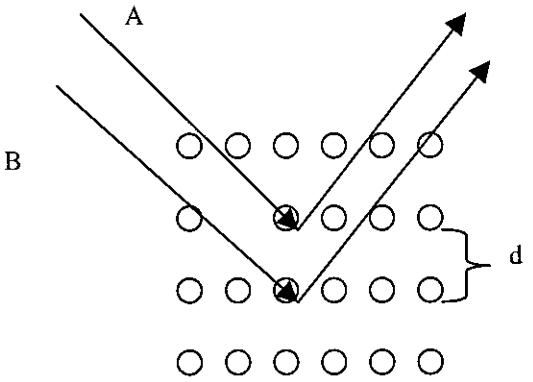

Figure 2. Schematic of interaction between x-ray and atom in the material.

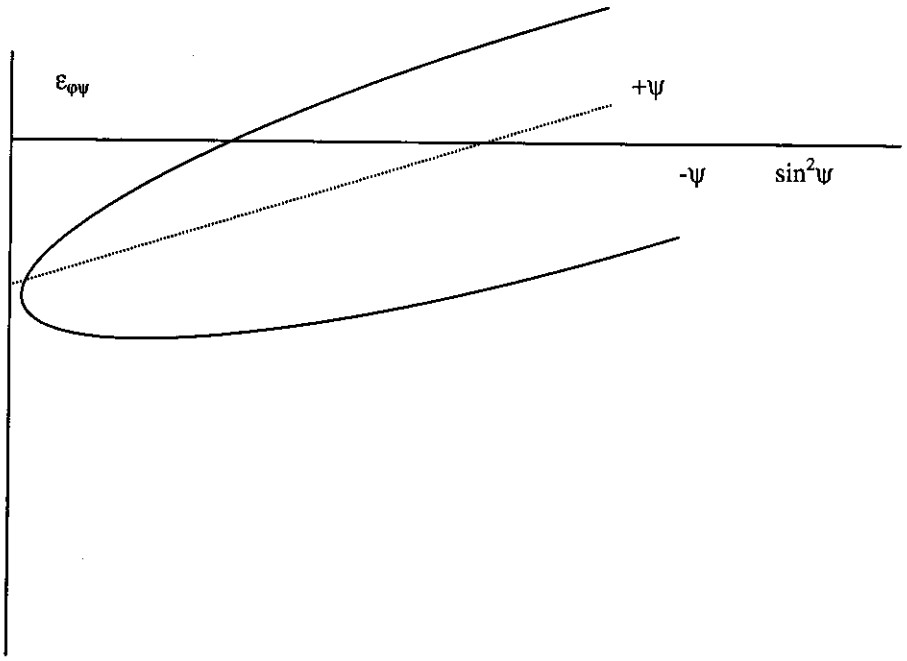

Figure 3. Typical plot of strain components $\varepsilon_{\varphi\psi}$ versus $\sin^2\psi$ measured by X-Ray Diffraction [5]

Table 2: Stress tensor for the sample with different deposition time.

Deposition time	σ_{11}	σ_{12}	σ_{13}	σ_{21}	σ_{22}	σ_{23}	σ_{31}	σ_{32}
1 hours	1784	-409	153	-409	-21	-112	153	-112
2 hours	183	128	17	128	-67	-19	17	-19
3 hours	1478	56	-128	56	1179	103	-128	103
4 hours	-148	870	126	870	803	88	126	88
5 hours	-36	89	0	89	-83	24	0	24

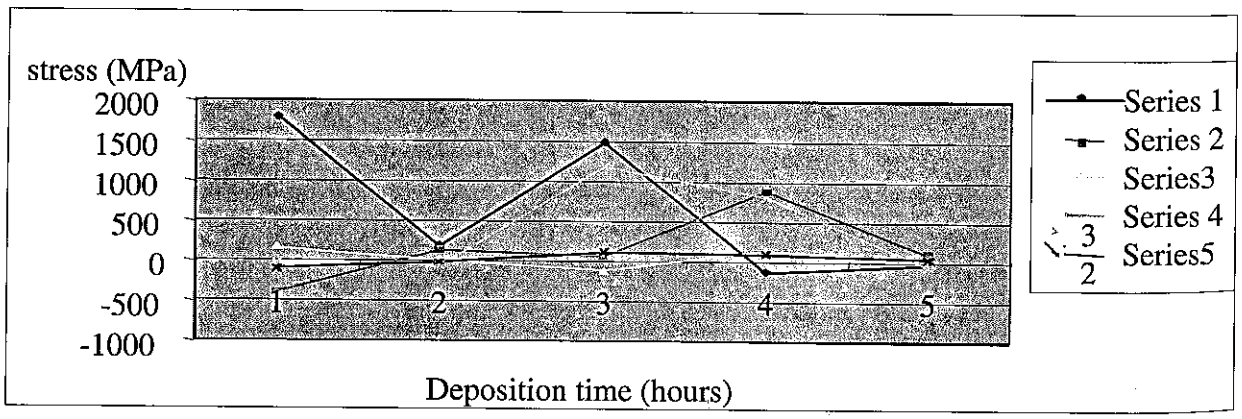

Figure 4. Influences of deposition time on the stress tensor in the cBN films

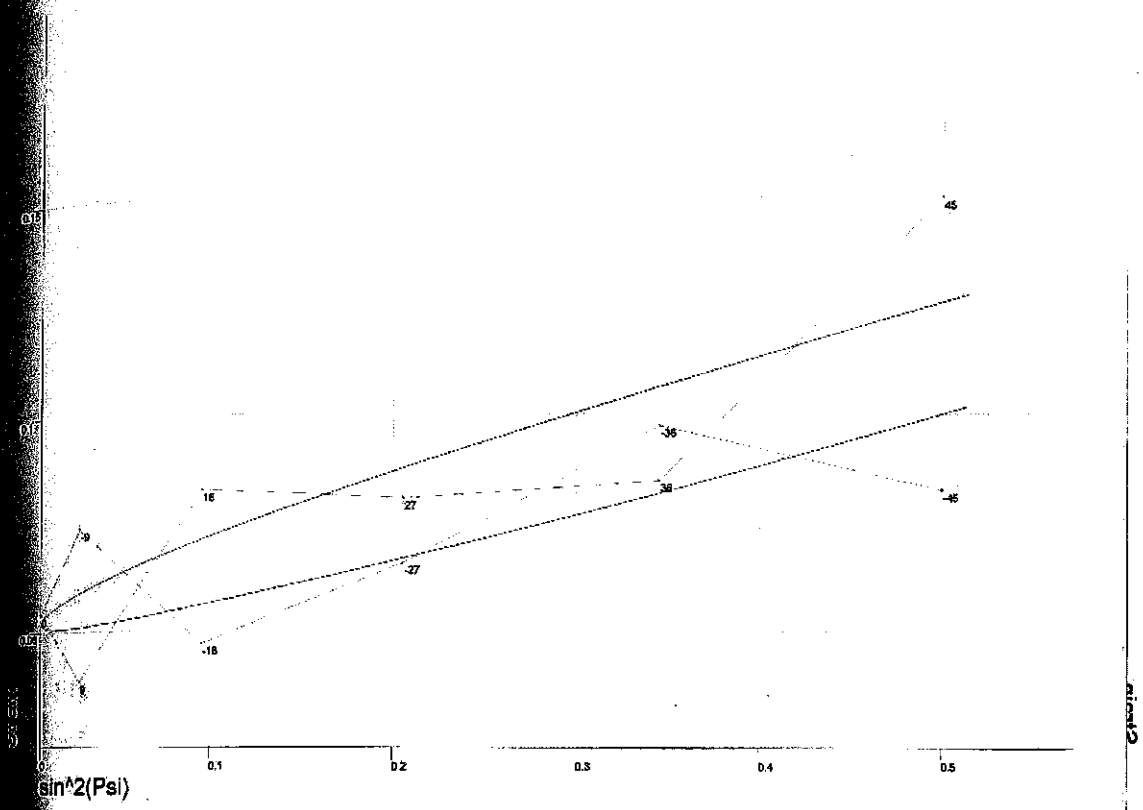

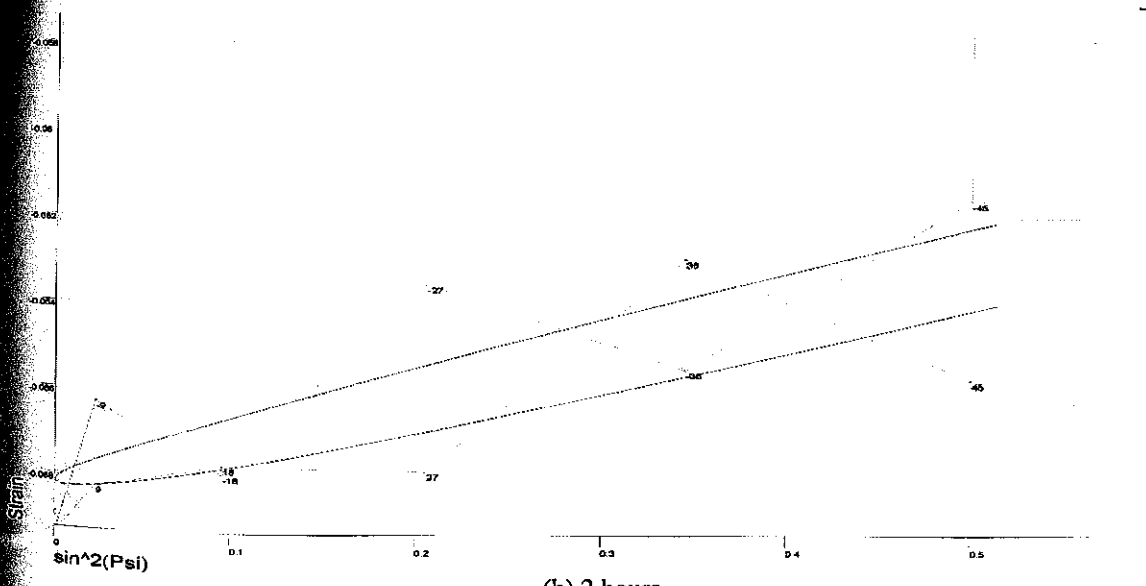

(b) 2 hours

Figure 5. Stress charts of the cBN films with different deposition time

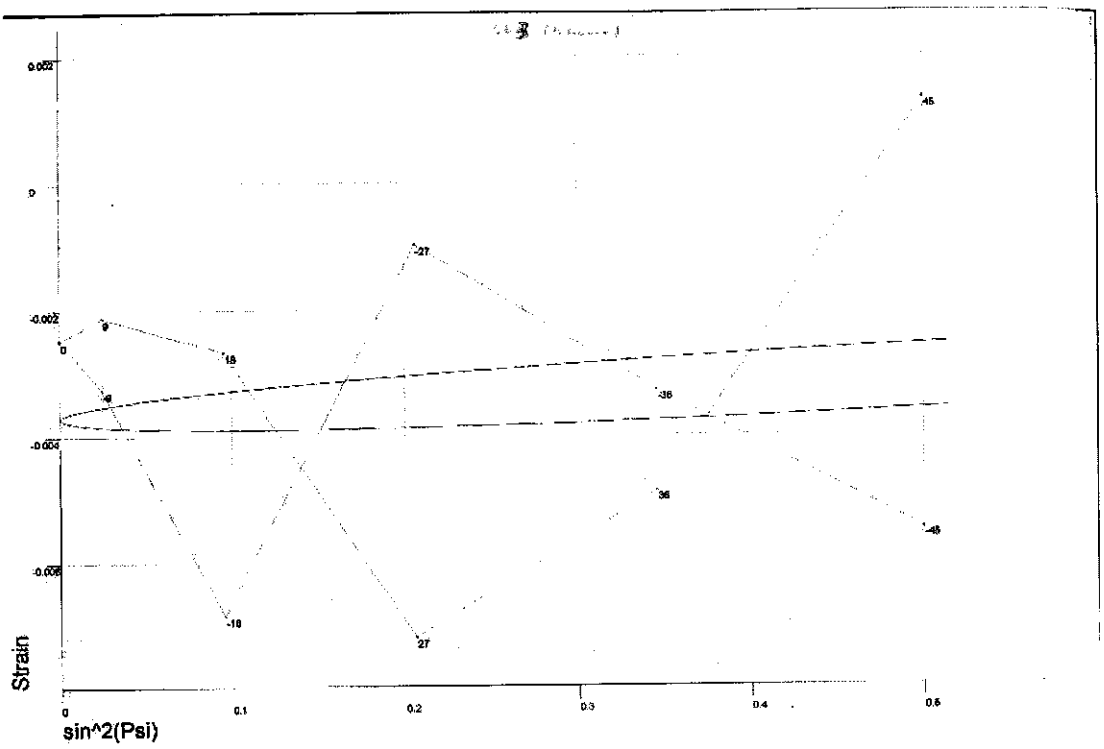

(c) 3 hours

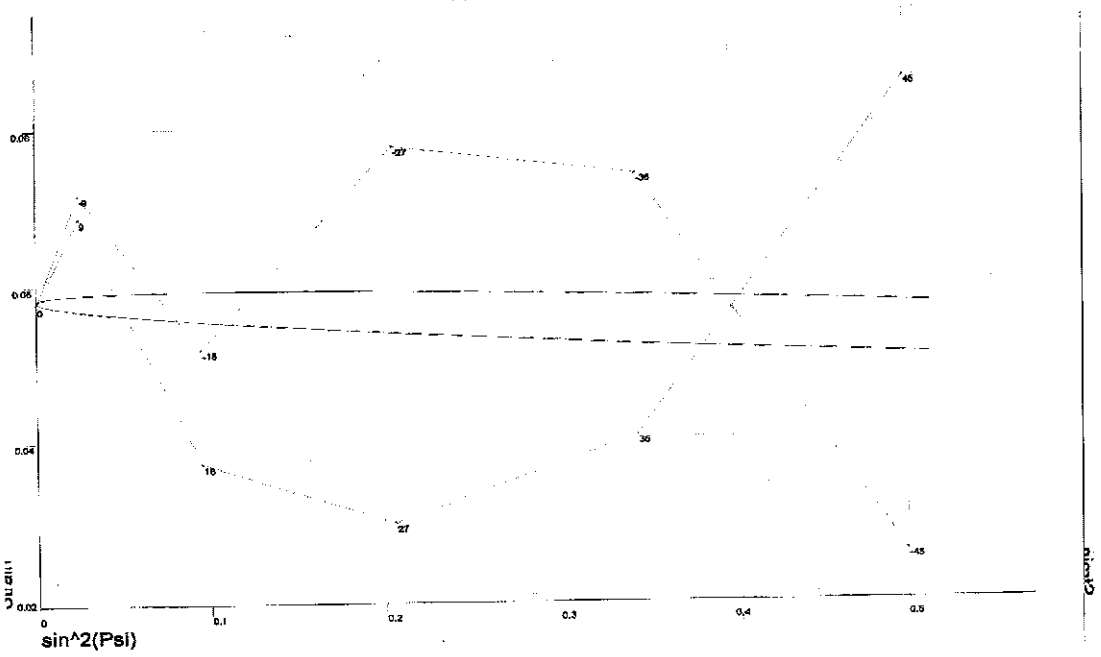

(d) 4 hours

Figure 5. Stress charts of the cBN films with different deposition time

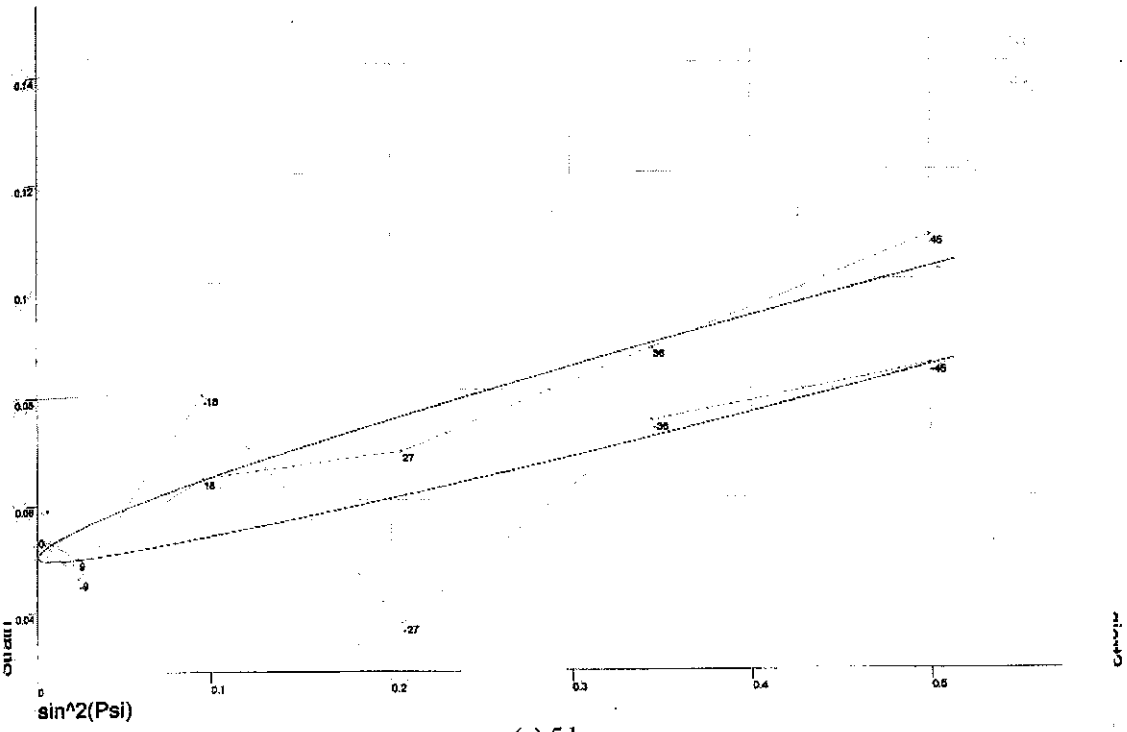

(e) 5 hours

Figure 5. Stress charts of the cBN films with different deposition time

Cubic Boron Nitride Films Growth by Rf Sputtering Process

In Rf sputtering process, most of the sputtered atoms consist of boron (B) and nitrogen (N) atoms, which will move individually towards the substrate. After B and N atoms arrive on the substrate, the first compound, which is formed, should be the compound, which has the energy of formation equal to the condition (which is determined by pressure and temperature) when B and N interacted for the first time on the substrate.

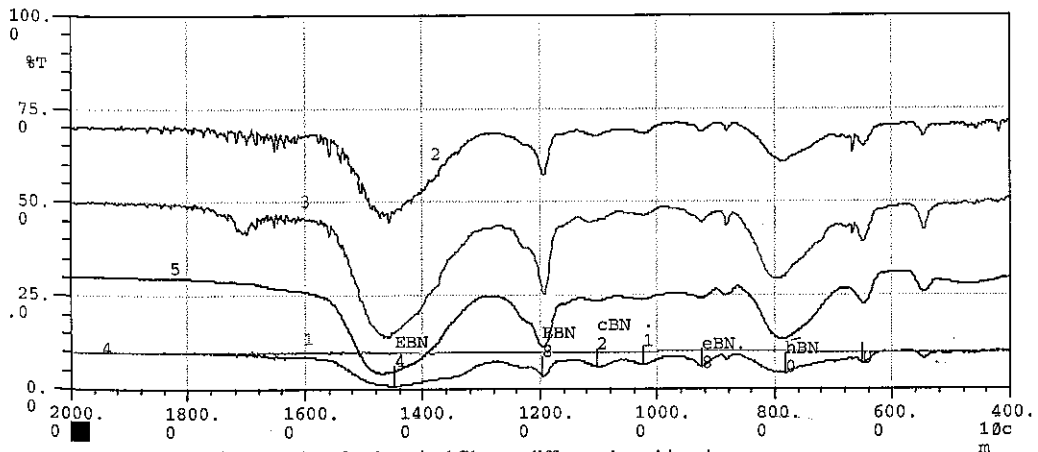

Figure 6. FTIR chart for deposited films at different deposition time.

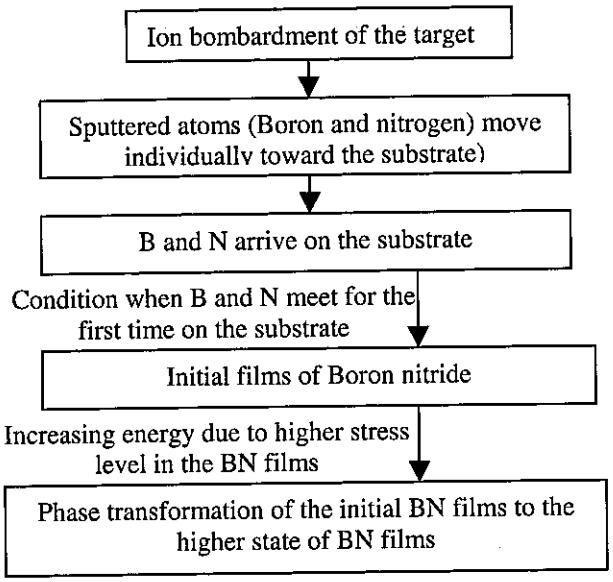

Figure 7. The proposed the growth of BN films by sputtering method.

According to Friedman [1], the energy for cBN transformation requires about one ion of energy 500 - 1000 eV for each deposited atoms, and since the energy of the sputtered atoms in this work is less than 32 eV, it seems impossible to form cBN phase from the first boron and nitrogen atoms coming on to the steel substrate. However from FTIR data in Figure 4, apart from hBN phase and E-BN, it was also found that cBN phase was also present in the deposited films. It is suggested that the interaction of the growing films with the next batch of sputtered atoms could result in the phase transformation of the growing films and the phase transformation can be increased with longer deposition time as shown in Figure 4. It shows that transmission peak characteristic of cBN transmission peak at 1103 cm^{-1}. The result also shows that longer deposition time will make the characteristic peak becomes more significant.

This condition is also the characteristic of martensitic transformation. It is suggested that martensitic transformation is the mechanism of cBN transformation. Therefore for longer deposition time there would be more phases transform to cBN.

McKenzie *et. al* [3] have found that large compressive stress, increases the effect of 'pressure' on BN and leads to the material transforming to cBN. On the other hand, Windschman [4] suggested that stress is proportional to the total number of displaced atoms and should scale linearly with energy for the formation of cBN. However we found that not all of the stress is responsible to the phase transformation to cBN. From Table 2, we can see that only stresses in certain direction (σ_{12} and σ_{21}) increased with increasing amount of cBN phases in BN films (Figure 6).

Friedmann *et. al* [1] proposed that quenching mechanism play an important role for the transformation to cBN phase. He also proposed that the number of defects or defect concentration is responsible for the transformation to cBN phase. Both of these factors are the characteristic of martensitic transformation, as proposed by Nishiyama [6]. In this sense, martensitic transformation is the proposed mechanism for cBN transformation. In addition, to confirm this theory, we suggested that the mechanism of transformation to the cBN phase is a cooperative movement of atoms, which occurs at certain direction. This is indicated by increasing of residual stresses only in certain direction of the BN film (it supposed that stress in the films is the driving force for the cBN transformation). Since the later condition is also the characteristic of martensitic transformation, it is suggested that martensitic transformation is the mechanism of cBN transformation. Figure 7 shows the proposed growth of cBN film by sputtering method.

CONCLUSIONS

Various boron nitride films have been deposited on the steel (HSS) substrate using Rf sputtering method. From stress measurement calculation by DIFFRAC^{plus} and confirmed by structure data from FTIR chart, it is suggested that stress in certain direction of the films can be the driving force for the formation of cBN phase. This is an indication that martensitic transformation is the typical transformation of

cBN phase, which were also suggested by other researchers.

REFERENCES

1. Friedmann et.al.(1994). *J.Applied Physic.* 76(5).Pg3088-3100.
2. Setsuhara et.al.(1997). *Nuclear Instruments and Methods in Physics Research B.* 127/128. Pg851-856.
3. McKenzie et.al.(1993). *Diamond and Related Material.* 2. 970.
4. Windischman H. (1991). *J. Vac. Sci. Technol.* A9,2431.
5. Bruker Advanced X-Ray Solutions. *Diffrac plus users manual.*
6. Nishiyama Z. (1978). *Martensitic Transformation.*